Pergamon

Journal of South American Earth Sciences, Vol. 9, Nos 1/2, pp. 91–109, 1996

0895-9811/96 $15.00 + 0.00

PII: S0895-9811(96)00030-2

Trace and rare-earth element characteristics of acidic tuffs from Southern Peru and Northern Bolivia and a fission-track age for the Sillar of Arequipa

[1]N. VATIN-PERIGNON, [1]G. POUPEAU, [2]R.A. OLIVER, [3]A. LAVENU, [1]E. LABRIN, [1]F. KELLER AND [1,2]L. BELLOT-GURLET

[1]Laboratoire de Géologie, URA 69 CNRS, Université Joseph Fourier de Grenoble, 15, rue Maurice Gignoux, 38031 Grenoble Cedex, France

[2]Institut Laüe-Langevin, BP 156, Avenue des Martyrs, 38042 Grenoble Cedex, France

[3]ORSTOM, UR 1H, 213 rue La Fayette, 75480 Paris Cedex 10, France et Laboratoire de géodynamique et modélisation des bassins sédimentaires, IPRA, Université de Pau et des Pays de l'Adour, avenue de l'Université, 64000 Pau, France

Abstract — Trace-element and REE data of glass and pumices of acidic tuffs and related fall deposits erupted in southern Peru and northern Bolivia between 20 and 0.36 Ma display typical characteristics of subduction related continental arc magmatism of the CVZ with strong LILE/HFSE enrichment and non enrichment of HREE and Y. Geochemical variations of these tuffs are linked to subduction processes and controlled by changes in tectonic regimes which occured with each Quechua tectonic pulse and affected the astenospheric wedge and both the dowgoing and the overriding lithospheres. During Neogene — Pleistocene times, tuffs erupted in northern Bolivia are typically enriched in Zr, Hf, Th, Ba, LREEs and other incompatible elements and incompatible /Yb ratios are much higher relative to those erupted from southern Peru, at a given SiO_2 content (65–67 wt. for dacites, 72–73 wt.% for rhyolites). Zr/Hf ratios increase eastward from 27 to 30 and Ce/Yb_N ratios from 11 to 19 reflecting the variation of degree of wedge contribution. Fractionation of the LREE over the HREE and fractionation of incompatible elements may be due to their heterogeneous distribution in the magma source. More highly fractionated REE patterns of Bolivian tuffs than Peruvian tuffs are attributed to variable amounts of contamination of magmas by lower crust. After the Quechua compressional event at ~7 Ma, Sr/Y ratios of tuffs of the same age, erupted at 150–250 km or 250–400 km from the Peru-Chile trench, increase from southern Peru to northern Bolivia. These differences may be attributed to the subduction of a swarm oceanic lithosphere under the Bolivian Altiplano, leading to partial melting of the sudbucted lithosphere. New FT dating of obsidian fragments of the sillar of Arequipa at 2.42± 0.11 Ma. This tuff dates the last Quechua compressional upper Pliocene phase (~2.5 Ma) and confirms that the sillar is not contemporaneous with the Toba 76 tuff or the Perez ignimbrite of northern Bolivia. Geochemical characteristics of tuffs erupted before and after this last compressional phase remained the same and provide evidence that the upper Miocene (~7 Ma) compressional deformations played the most important role on the variability of the geochemical characteristics of the southern Peruvian and northern Bolivian tuffs. Copyright © 1996 Elsevier Science Ltd & Earth Sciences & Resources Institute

INTRODUCTION

In the Central Andes, large volumes of Neogene acidic tuffs cover large areas of the Altiplano of Bolivia and the Puna of northern Chile and Argentina. These have been extensively studied by numerous workers (see Schmitt-Riegraf and Pichler, 1988; de Silva, 1989, de Silva and Francis, 1989 and refs. therein). Magmas of these voluminous silicic pyroclastic flow deposits are considered as the response to uplift and thickening of the crust during different tectonic pulses (Isacks, 1988; de Silva, 1989, de Silva and Francis, 1991). A variety of models have been proposed for the genesis of these silicic magmas, including crustal anatexis and combined assimilation-fractional crystallization processes and (*e.g.* Thorpe *et al.*, 1979, Francis *et al.*, 1980, Hawkesworth *et al.*, 1982, James, 1984, Harmon *et al.*, 1984), melting, assimilation, fractionation and homogenization (MASH) processes (Davidson *et al.*, 1990, Davidson and de Silva, 1992) and large scale of melting of middle to lower continental crust, perhaps in association with lithospheric thinning (Hawkesworth and Clarke, 1994, Francis and Hawkesworth, 1994).

Our study is focused on some tuffs and fall deposits related to the subduction of the Nazca plate beneath western South America in the Andean Central Volcanic Zone (CVZ, Thorpe *et al.*, 1984) between 15°S and 18°S. These tuffs were emplaced during Neogene and early Quaternary times (Early Miocene to Pleistocene) in the Pacific piedmont and the south of the western Cordillera in Peru and in the northern part of the Altiplano and the eastern Cordillera piedmont (La Paz and Titicaca basin) in Bolivia. A detailed discussion of the geochronological evolution of this part of the Bolivian Central Andes based on new K-Ar ages from volcanics including some of these tuffs is given in a previous work (Lavenu *et al.*, 1989). The specific goals of the present study are to provide a description of the physical and chemical characteristics of these tuffs and to interpret their geochemical variations in terms of the source region and their tectonomagmatic significance in the context of changes in tectonic regimes of the southern Peruvian and northern Bolivian Andes between 20 – 0.3 Ma. In addition, new fission track (FT) ages of three obsidian fragments from the sillar of Arequipa are presented and discussed here, because these tuffs have important geotectonic implications.

GEOLOGICAL BACKGROUND

Tuffs and related fall deposits of the CVZ, between 15°S and 18°S, are found along a west-east geographic

traverse beginning in the Arequipa Province and continuing into the northern Bolivian Altiplano (Fig. 1). These tuffs are divided in four groups belonging to the main units of the morphostructural zoning of this part of the Central Andes. These paleogeographic domains are, from west to east, the Pacific piedmont (coastal range) and the western Cordillera (high volcanic arc) in southern Peru, the Altiplano and the eastern Cordillera in northern Bolivia (La Paz and Titicaca basin on the western flank of the eastern Cordillera). The study area is located 150 to 300 km from the Peru-Chile trench axis over a moderately dipping segment of the subducted Nazca plate (average 25°-30° E from 25- to 100-km depth) and about 100–130 km above the top of the seismic zone. The crustal thickness is about 70 km beneath the western Cordillera and the western part of the Altiplano and 50–55 km beneath the eastern Cordillera. The subducted lithosphere is separated from the continental crust by a well-developed wedge of astenospheric mantle (Grange *et al.* 1984)

A compilation of available K-Ar dates has provided a geochronology upon which the tectonic evolution of these regions has been assessed by various authors (*e.g.* Tosdal, 1981; Bellon and Lefévre, 1976; Noble *et al.*, 1985). More recently, new K/Ar dates on undeformed or slightly folded tuffs from northern Bolivia after 10 Ma and their lithological position was discussed in detail by Lavenu (1986) and Lavenu *et al.*, (1989) and a revised stratigraphy for the SW Peru has been established by Sébrier *et al.*, (1988). Four phases of explosive volcanism can be considered, using the geological time scale of Odin (1994): 1) the early Miocene sequences 20.3 – 15.8 Ma) from the Pacific piedmont and the western Cordillera, 2) the middle to late Miocene sequences (9.1 – 5.5 Ma) from the western Cordillera, the Altiplano especially with the well-known tuff so-called the Toba 76 tuff and the lower part of the La Paz and Titicaca basin, 3) the Pliocene sequences (5 – 2 Ma) which are present in all the chain and its piedmont especially the Perez ignimbrite in Bolivia and 4) the Pleistocene sequences (1.6 – 0.4 Ma) with tuffs interbedded within formations of the upper Barroso Formation in Peru and contemporaneous of glaciations in Bolivia. The chronology shows that this explosive activity appears to have been significantly reduced between 15 and 10 Ma but continued to be important from the late Miocene until recently (eruption of the Huaynaputina volcano, east of Arequipa, on February 18, 1600; Torbio, 1899).

The stratigraphic positions and age determinations of tuffs and related fall deposits analysed in this study from the western Cordillera piedmont in southern Peru to the eastern Cordillera piedmont in Bolivia (La Paz and Titicaca basin) are given in Table 1.

Stratigraphy and New Fission-track (FT) Age of the Sillar of Arequipa

The well-known rhyolitic ash-flow tuff, so-called the "*sillar*" of Arequipa (SA tuff) by Fenner (1948) is considered as a nonwelded ignimbritic tuff (Jenks and Goldich, 1956). This tuff infilled the valleys and was also deposited on relative flat surfaces. It is one of the most interesting tuffs of the Arequipa Province due to its use as a building stone. Lefévre (1979) recognized the high content of juvenile fragments and the widespread vertical (up to 200 m thick) and lateral area of dispersal of the SA tuff and observed the presence, but not everywhere, of compaction and welding of pumiceous fragments. A quarry located along the Quebrada Añas Huayco at the northwestern edge of the town of Arequipa shows a partial section of the SA tuff. The base is not exposed and the visible section consists at least of two ash-flow units with a total thickness of about 10 m. The working of the quarry aids the recognition of a fine-grained layer at the base of the upper flow unit suggesting different eruptive pulses (Sparks *et al.*, 1973) difficult. The SA tuff could have been an emplacement during a single volcanic episode or a series of events in rapid succession (Fig. 2A and B).

The lower flow unit (3–4 m thick) is a lithic-rich and well indurated tuff. At the base, both white and oxidized fibreous and vesicular glassy pumices and glass fragments all tend to be small. Towards the top of this unit, the pumices increase in size ($\sim$ 10–15 cm) and relative abundance. Lithic clasts (up to 25%) are concentrated particularly at the base of the unit and consist mainly of subrounded oxidized andesite fragments ($\sim$ 5 cm) of the underlying lower Barroso formations. Isolated crystals of plagioclase, biotite and magnetite are abundant in the fine- to medium-grained pumiceous and ashy matrix.

The upper flow unit (6 m exposure in the quarry) is an indurated, homogeneous, pumice-rich (30%) rhyolitic tuff which shows large columnar joints indicating emplacement at a high temperature. The matrix is fine-grained, crystal and lithic clast-poor ($\sim$ 10%, Fig. 2 C). Grey to yellow glassy pumices are fragile, highly vesiculated and their phenocryst content is low ($\sim$ 5%). Coarse pumices occur at the top of this unit. The matrix is crystal-rich with large plagioclase, biotite, Fe-Ti oxides as well as apatite and rare hornblende. Obsidian glass fragments (SA1–90, SA2–90 and SA3–90) are abundant and petrographically identical to pumices.

The top of the SA tuff is separated from an overlying salmon-pink tuff by an irregular erosion surface. This tuff in turn is overlain by glacial conglomerates, coarse fluvial gravels and lahars which cap the mesa in the Arequipa area.

Fission-track Dating of Obsidian Samples of the SA Tuff

The FT analytical procedure is described in the appendix and analytical data are summarized in Tables 2 and 3. Track size analysis, as reported in Table 2 and illustrated in Fig. 3, shows that in the three samples measured, fossil spontaneous fission tracks are, on the average, 20% shorter than induced tracks, indicating

SAES 9:1/2-6

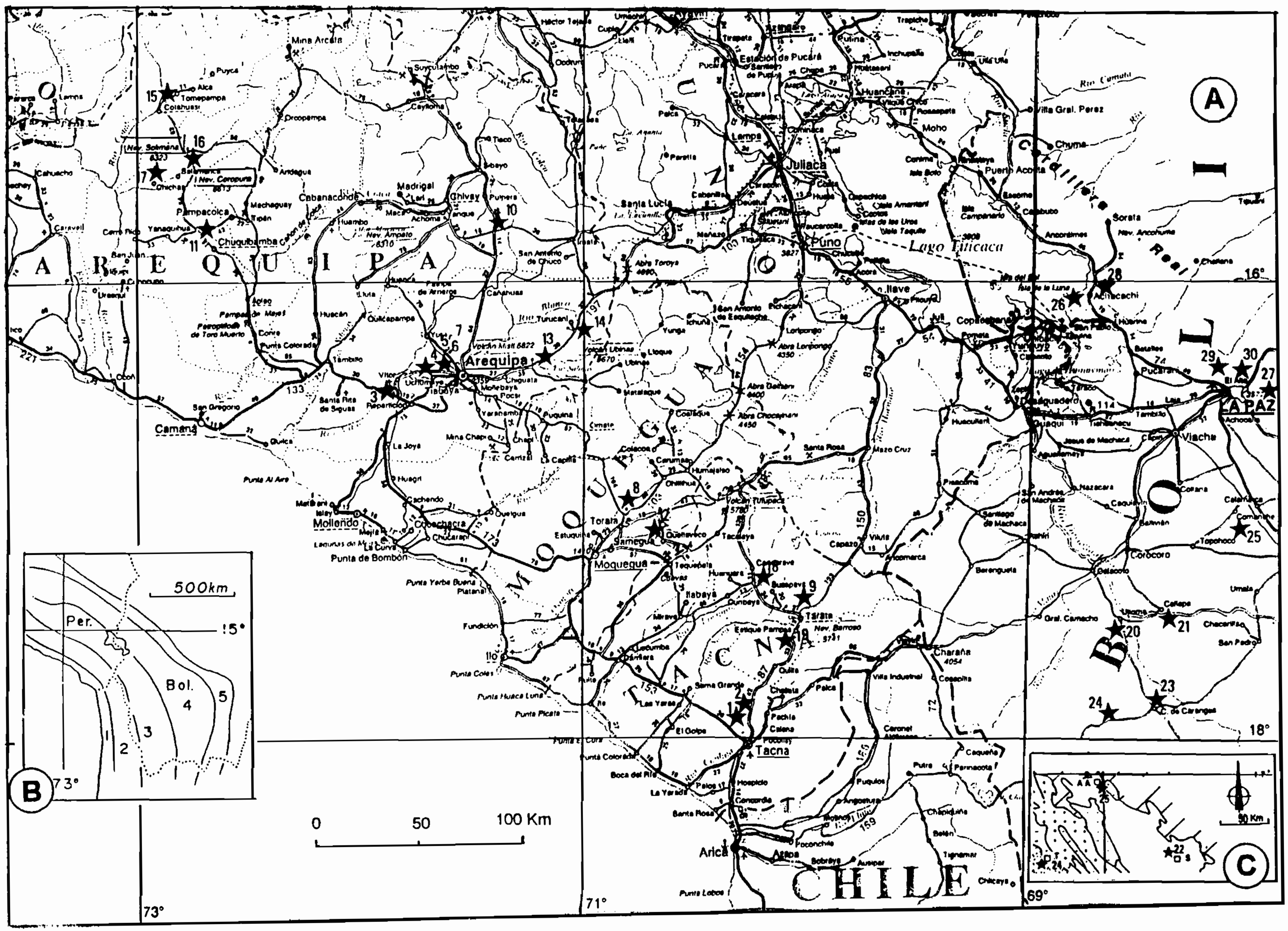

Fig.1. Index map of Central Andes (southern Peru-northern Bolivia) between 68–73°W and 15–18°S. A: numbered stars indicate sample localities (see Table 1). B: morphostructural zonation of Central Andes. 1: coastal Cordillera and Pacific piedmont; 2: western Cordillera; 3: Altiplano; 4: eastern Cordillera; 5: subandean zone. Bol: Bolivia; Per: Peru. C: location of sample 22, the Soledad tuff (S), east of Tirata (T) and south-east of Ayo Ayo (AA) in Bolivia after the simplified geological map of Lavenu *et al.* 1989.

Table 1 Location and age determinations of acidic tuffs from southern Peru and northern Bolivia according to various authors. Letters and numbers quoted referred to samples dated by authors cited in reference.

N°	Sample	Location (Lat.S, Long. W)	Altitude (m)	Unit	Method	Age (Ma)	References
Peruvian Pacific Piedmont							
	185	Alto de la Alianza 17°59' - 70°15'	770	Huaylillas Fm.	K/Ar	18.4±0.5	Bellon and Lefèvre, 1976
1	Pe3	Alto de la Alianza 17°59' - 70°15'	770	Huaylillas Fm.	K/Ar	20.3±0.8	Feraud in Sébrier et al., 1988
	186	Alto de la Alianza 17°57' - 70°15'	920	Huaylillas Fm.	K/Ar	18.35±0.5	Bellon and Lefèvre, 1976
2	Pe2	Alto de la Alianza 17°57' - 70°15'	920	Huaylillas Fm.	K/Ar	19.2±0.8	Feraud in Sébrier et al., 1988
3	Pe53	Rio Vitor,Qda del Impertinente 16°27' - 71°57'	1200	lower Barroso Gr.	K/Ar	2.76±0.1	Bonhomme in Vatin-Pérignon et al, 1982
	silfer	Qda de la Gloria 16°31' - 71°46'	1800	lower Barroso Gr.	K/Ar	3.05 - 3.4	Taupinard in Laharie and Derruau, 1974
4	Pe32	Qda El Cuico, Arequipa 16°19' - 71°42'	2400	lower Barroso Gr.	K/Ar	2.9±0.1	M.G. Bonhomme, Grenoble, unpublished data
5	SA1-90	Qda Añas Huayco, Arequipa 16°20' - 71°35'	2520	lower Barroso Gr.	FT	2.32±0.21	this study
6	SA2-90	Qda Añas Huayco, Arequipa 16°20' - 71°35'	2520	lower Barroso Gr.	FT	2.43±0.24	this study
7	SA3-90	Qda Añas Huayco, Arequipa 16°20' - 71°35'	2520	lower Barroso Gr.	FT	2.48±0.17	this study
Peruvian western Cordillera							
8	Pe29	Alto de Tala, Moquegua 17°05' - 70°41'	3810	Huaylillas Fm.	K/Ar	18.6±0.7	Feraud in Sébrier et al., 1988
9	Pe17	Pampa de Tintinave, laguna Aricota 17°24' - 70°09'	2940	Tacaza Fm.	K/Ar	15.8±0.6	Feraud in Sébrier et al., 1988
10	Pe52	Callali, rio Llapa, 15°30' - 71°25'	3900	Tacaza Fm.	K/Ar	8.9±0.7	Feraud in Sébrier et al., 1988
11	Pe44	Qda de Rata, Chuquibamba 15°45' - 72°43'	3950	lower Barroso Gr.	K/Ar	6.0±0.2	Feraud in Sébrier et al., 1988
12	Pe23	Quellaveco Mine 17°06' - 70°30'	3800	lower Barroso Gr.	K/Ar	5.1±0.2	Feraud in Sébrier et al., 1988
13	Pe33(=51)	Infiernillo, Laguna Salinas 16°16' - 71°04'	4300	lower Barroso Gr.	K/Ar	4.45±0.3	Bellon and Lefèvre, 1976
14	Pe42	Co Pan de Azucar, Ichuña 16°02' - 71°54'	4600	upper Barroso Gr.	K/Ar	1.8±0.2	Feraud in Sébrier et al., 1988
15	PH1-79c	Co Huiñao, Cotahuasi 15°13' - 72°52'	2880	upper Barroso Gr.	K/Ar	1.9±0.2	Feraud in Sébrier et al., 1988
	silfer	Co Quiroz, Yanaquihua 15°46' - 72°53'	2850	upper Barroso Gr.	K/Ar	1.8±0.5	Weibel et al., 1978
16	80-109	Campamento Sique, Nevado Corupuna 15°30' - 72°45'	4525	upper Barroso Gr.	K/Ar	1.8±0.2	Feraud in Sébrier et al., 1988
	Ignimbrite	Acoypampa Grande 15°46' - 72°45'	3950	upper Barroso Gr.	K/Ar	1.7±0.2	Weibel et al., 1978
17	80-104	Co Chachane, Nevado Solimana 15°31' - 72°55'	3800	upper Barroso Gr.	Rb/Sr	1.46±	L. Briqueu, Montpellier, unpublished data
18	Pe18	Yucamane Pampa, Candarave, rio Callazas 17°150' - 70°14'	3200	Sencca Fm.	K/Ar	0.97±0.04	M.G. Bonhomme, Grenoble, unpublished data
19	Pe8	Estique Pampa, Pachia 17°32' - 70°02'	2900	Sencca Fm.	K/Ar	0.36±0.01	Bonhomme in Vatin-Pérignon et al, 1982
Bolivian Altiplano							
20	PH64 (=IJ)	Upper Tinajani , Ulloma tuff 17°29' - 68°30'	3800	Totora Fm.	K/Ar	9.1±	Evernden et al., 1966, 1977
21	PH61 (=II)	Upper Tinajani , Callapa tuff 17°27' - 68°22'	3780	Mauri Fm.	K/Ar	8.2±	Evernden et al., 1966, 1977
22	PH48	Co Pucara, Soledad tuff 17°41' - 67°19'	3760	Umala Fm.	K/Ar	5.2±0.3	Lavenu et al., 1989
	SR504	Chillcani Pampa, Soledad tuff 17°49' - 67°18'	3750	Umala Fm.	K/Ar	5.8±0.2	Redwood and MacIntyre, 1989
23	BO9 (=IC)	Estancia Chiriquiña, Toba 76 tuff 17°49' - 68°22'	3940	Umala Fm.	K/Ar	5.4±	Evernden et al., 1966, 1977
24	BO7	Estancia Tirata, Pastara, Perez Ignimbrite 17°53' - 68°36'	4100	Perez Fm.	K/Ar	3.3±0.3	Lavenu et al., 1989
25	LA82-2	Ayo Ayo and Villa Remedios, Ayo Ayo tuff 17°07' - 67°59'	3900	Umala Fm.	K/Ar	2.8±0.4	Lavenu et al., 1989
La Paz and Titicaca basin.							
26	LA82-1	Titicaca lake, Chua tuff 16°10' - 68°44'	3900	Umala Fm.	K/Ar	7.6±0.7	Lavenu et al., 1989
27	MB161	Cota Cota tuff 16°32' - 68°03'	3520	La Paz Fm.	K/Ar	5.5±0.2	Lavenu et al., 1989
28	PH54	Co Caballo, Chijini tuff 16°08' - 68°38'	3870	La Paz Fm.	K/Ar	2.8±0.07	Lavenu, 1986
29	MB153	Limanpata, rio Kaluyo, Patapatani tuff 16°25' - 68°07'	4160	La Paz Fm.	K/Ar	2.7±0.1	Lavenu et al., 1989
30	PH53a	Chuquiaguillo, Calvario Drift, Purapurani tuff 16°27' - 68°06'	4100	Patapatani Fm.	K/Ar	1.6±0.1	Lavenu et al., 1989

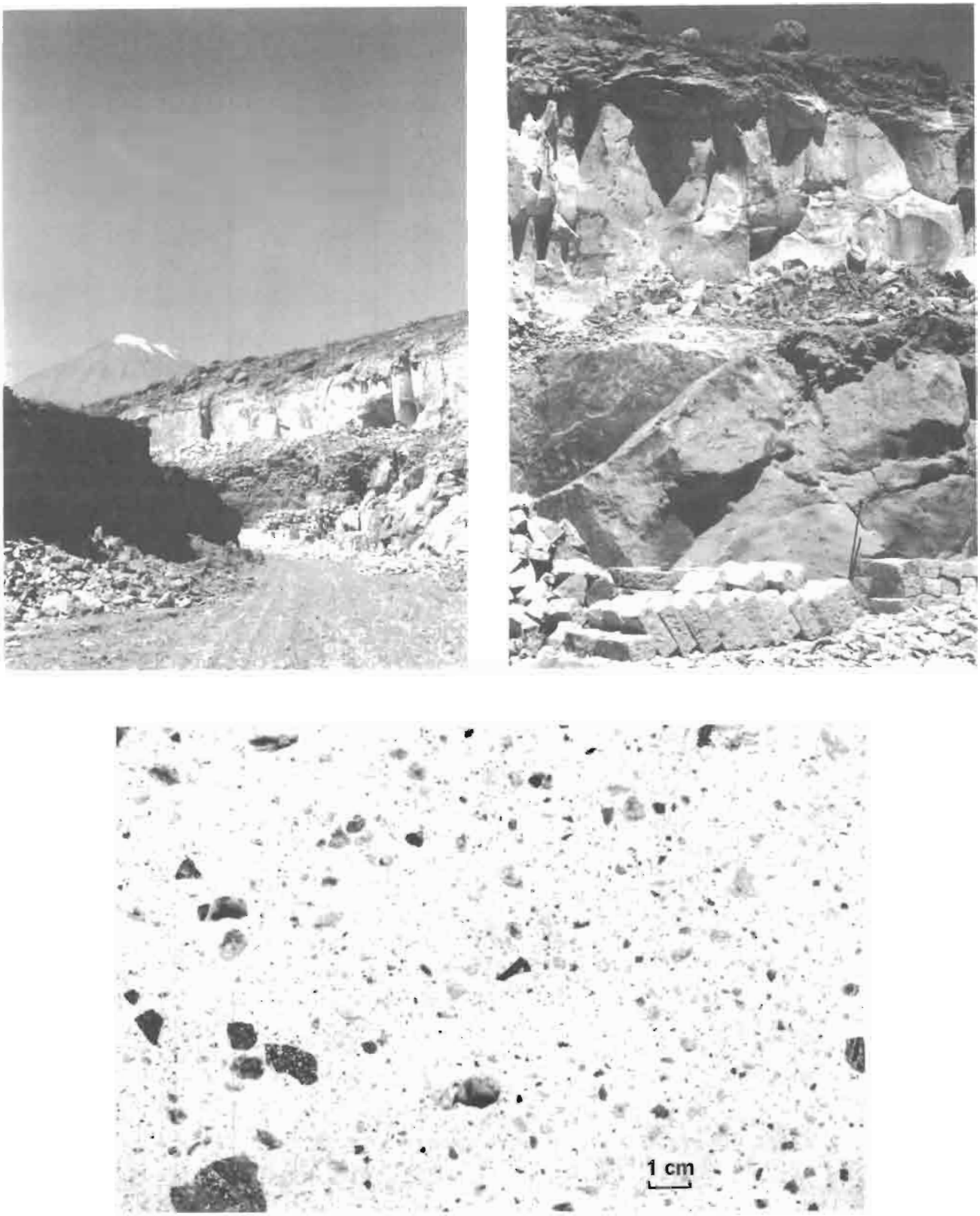

Fig. 2. A: southeast wall of the Quebrada Añas Huayco near the Arequipa airport showing the two flow units of the "*sillar*", the hand-cut building blocks and the southern slopes of the volcan El Misti (16°18×S-71°24×W, 5822 m) behind the quarry. B: detail of the pink-colored flow unit beneath the light-colored pumice-rich and columnar jointed flow unit of the "*sillar*" (SA tuff). C: polished section of a typical hand-cut building stone of the "*sillar*" of Arequipa.

natural track fading. The apparent fission track ages of the sillar glasses are therefore meaningless and some correction procedure has to be applied. We used the Storzer and Poupeau (1973) plateau technique, which consists, by submitting both an irradiated and an unirradiated glass fragment to a convenient thermal procedure before track etching, to reduce the fossil and induced track populations to the same degree of

Table 2 Track diameter analysis in Sillar glasses. **N** and d: number of measured tracks and mean track diameters, respectively. S and i refer to spontaneous and induced tracks. The reported uncertainties on d are the standard errors of the mean.

Sample	thermal treatment	Ns	ds µm	±1σ	Ni	di µm	±1σ	ds/di	±1σ
SA1-90	no	123	3,73	0,05	154	4,69	0,05	0,80	0,01
	2h.205°C	99	3,17	0,05	213	3,03	0,03	1,05	0,02
SA2-90	no	109	3,52	0,06	119	4,39	0,06	0,80	0,02
	2h.205°C	3	3,01	0,06	213	3,10	0,04	0,97	0,02
SA3-90	no	78	3,68	0,07	118	4,52	0,05	0,81	0,02
	2h.205°C	130	3,13	0,05	214	3,03	0,03	1,03	0,02

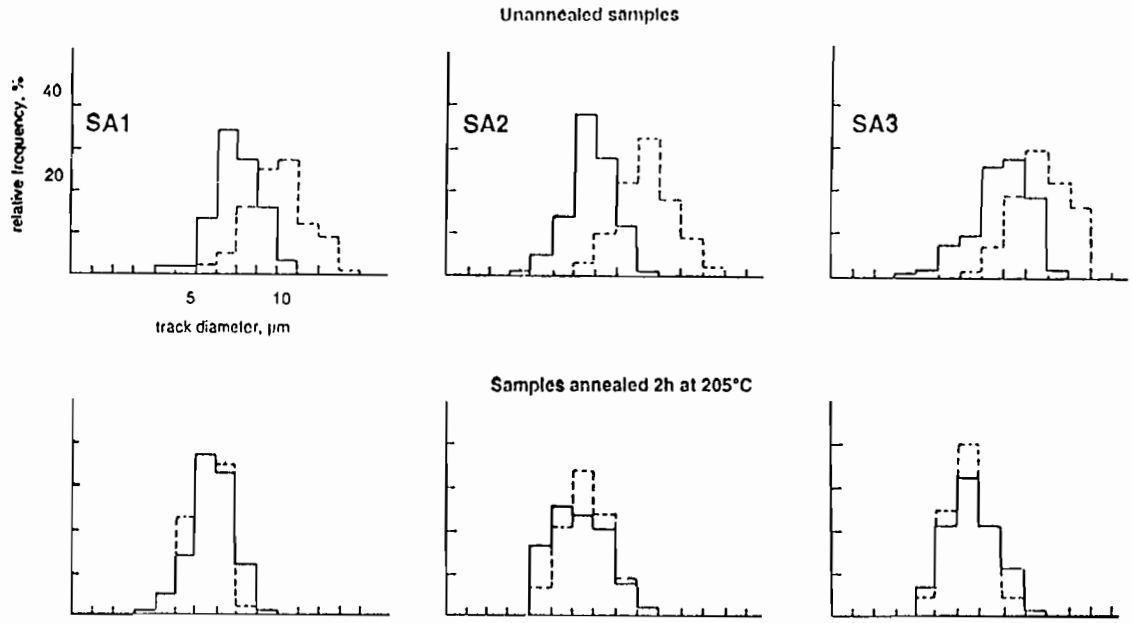

Fig. 3. Fossil (full lines) and induced (stippled lines) fission track diameter distribution in the 3 obsidian glass clasts dated, SA1, SA2 and SA3. Top: without any laboratory thermal treatment, fossil tracks appear as shortened relative to induced tracks due to natural fading. Bottom: samples were heated for 2 hours at 205°C before track etching. Fossil and induced tracks were reduced in size, although differentially and they now present similar track diameter distributions.

annealing, hence the same size distribution (Poupeau *et al.*, 1994, Dorighel *et al.*, 1994). It can be seen from Table 2 and Fig. 2 that a thermal treatment of 2 hours at 205°C was sufficient to reduce in the SA obsidian fragments the fossil and induced tracks to the same mean diameter and diameters distribution.

The apparent ages of the samples (Table 3) range from 1.19±0.10 Ma (SA2–90) to 1.42±0.11 Ma (SA3–90). The track size analysis having shown that fossil tracks were affected by some natural fading, these ages are only lower estimates of their formation ages. After a thermal treatment at 205°C, fossil and induced track have reached similar size distribution. Electron microprobe analyses revealed the glass in the SAtuff is chemically homogeneous. The three samples analysed, SA1–90, SA2–90 and SA3–90 present concordant "plateau" ages, at respectively 2.32±0.21 Ma, 2.43±0.24 Ma and 2.48±0.17 Ma (1s). We therefore adopt for the sillar of Arequipa the weighted mean age of *2.42±0.11 Ma* (1s).

Table 3 FT dating of Sillar glasses. Analytical data.

Sample	Mic.	Thermal treatment	Ns	ns	Ds 10E3 t/cm²	±1σ	N(s+i)	n(s+i)	Di 10E3 t/cm²	±1σ	t app. Ma.	±1σ	t pl Ma	±1σ
SA1-90	1	no	198	990	1,51	0,11	2080	170	91,0	2,0	1,36	0,10		
	2	2h. 205°C	139	920	1,42	0,12	1094	200	50,2	1,5			2,32	0,21
SA2-90	1	no	151	800	1,43	0,12	2372	180	98,2	2,0	1,19	0,10		
	2	2h.205°C	123	855	1,36	0,12	1305	260	45,9	1,3			2,43	0,24
SA3-90	1	no	177	880	1,52	0,11	2126	180	87,8	1,9	1,42	0,11		
	2	2h.205°C	157	1040	1,42	0,11	2415	470	47,0	1,0	1,32	0,06	2,46 2,40	0,21 0,13

mic: microscopes. 1: Orthoplan Leitz; 2: Jenavert Zeiss Jena

N, n and D, respectively total number of tracks counted, of counts, and track densities. The s and i refer to respectively spontaneous and induced tracks.

tapp and tpl, apparent and plateau ages. FT ages were calculated using the equation $t=[D_S/(D_{(s+i)}-D_S)](\sigma I\Phi/\lambda)$, where $D_{(s+i)}$ is the track density measured in the irradiated fragment. $\sigma=580.2\times10^{-24}$ cm^{-2}; $I=7.253\times10^{-3}$; $\lambda=7.03\times10^{-17}$ years^{-1}.

The precision on a FT age depends primarily on the precision on the density ratio of the above equation. It has been derived as (Bigazzi 1986):

$$\sigma t/t = [1/N_S + 1/N_{(s+i)}]^{1/2} \times [D_{(s+i)}/D_i]$$

Weighed ages and uncertainties in the last line of the table were computed as:
$\sigma^2 = 1/\Sigma[1/\sigma_{tj}]^2$ and $t = \Sigma[t/(\sigma_{tj})^2]/\Sigma[1/\sigma_{tj}^2]$

Brief Description of Other Tuffs

Southern Peru. In the Arequipa area, two rhyolitic pumice flow deposits (Pe32 and Pe53) are sandwiched between Pliocene conglomeratic layers of the Pacific Piedmont. These tuffs developed columnar joints and filled river valleys. Pe53 has given a feldspar age of 2.76±0.1 Ma (Vatin-Pérignon *et al.*, 1982) which disagree with ages of 3.05 reported by Laharie and Derruau (1974).

The Huaylillas Formation occurs along the Pacific Piedmont and in the western Cordillera and consists mainly of tuffs that have yielded lower Miocene ages. Sequences of rhyolitic flows and falls erupted between 18.6 and 18.3 Ma have been sampled in various localities: Alto de la Alianza (Pe3 and Pe2) and Alto de Tala, NE of Moquegua (Pe29). The oldest Miocene dacitic tuffs occur in the area of the laguna Aricota (Pampa de Tintinave, Pe17) and contain large quartz, and plagioclase, biotite, amphibole and Fe-Ti oxides in an abundant grey fine matrix of glass and feldspar. Near Callalli, the 8.9 Ma-old Sibayo tuffs (Pe52) of the Tacaza Group are well exposed in the rio Llapa valley. The most complete section is composed of three units separated by layers of river gravels. The lowest unit is a 20 m thick tuff with abundant lithics and basement clasts in a coarse-grained matrix containing pumices and crystals of quartz, plagioclase and biotite. The other two dacitic pyroclastic flow units consist of a well-indurated pumiceous tuff with well-developed columnar jointing (50 m thick) underlying a more vesiculated upper flow unit (30 m thick) containing abundant dacitic fragments. These three units are separated by thin layers of fluvial gravels. Tuffs of the Plio-Pleistocene group (Barroso Group) are well represented by dacitic tuffs near Chuquibamba (Pe44). At Quellaveco Mine, rhyolitic tuffs (Pe23) consist of two flow units and an overlying rhyolite lava flow. The lower unit corresponds to a ground surge deposit and the upper unit is a crystal-rich rhyolitic tuff with plagioclase, bipyramidal quartz and biotite in a pumiceous matrix. In the Laguna Salinas region, tuffs (Pe33) are very similar to those of the Moquegua region but the upper rhyolite lava flow is better developed. The young tuff of the Pan de Azucar (Pe42) consists of two pyroclastic flow units separated by

thin (10–20 cm) laminated pyroclastic surge deposits. The lower member is a single, thick (over 30 m), nonwelded, homogeneous unit and the upper member, with a thickness of about 10 m, is a indurated unit with numerous vitrophyric fiamme. The large tuff deposits of the upper Barroso Group are an extensive and stratigraphically important horizon of at least 500 m thick in the Cotahuasi graben (PH1–79c). The formation consists of a lower welded flow unit which varies in thickness from 55 to 75 m. Basal vitrophyre and fiamme are common with small lithic fragments and rare pumices. The matrix is fine-grained and contains plagioclase, amphibole and ubiquitous oxides. The upper unit is typically a pink welded tuff with small white pumices and abundant lithics. The two units are columnar jointed . The uppermost member of this series is visible near Allahuay and consists of a pumiceous nonwelded flow unit underlying Plinian airfalls. The 0.97 Ma-old tuff (Pe18) is found filling in a river valley near the Yucamane volcano. This nonwelded single flow unit of about 30–50 m thick contains abundant pumice blocks. The youngest Pleistocene tuff (Pe8) is an homogeneous, grey andesite of limited extent with relatively dense pumices and well-developed columnar joints.

Northern Bolivia. The Altiplano pyroclastic formations correspond to tuffs of the Totora and Umala Formations (Lavenu, 1986). The Ulloma tuff (PH64) is an homogeneous, pumice-rich, with pumices of all sizes dispersed in a fine-grained matrix containing dominant quartz and plagioclase with small amounts of biotite and amphibole. The Callapa tuff (PH61) is a pumice pyroclastic layer, reworked and/or weathered, with a crystal-poor matrix. The Soledad tuff (PH48), located northwest of Oruro, has been described in detail by Redwood (1987) and interpreted as a sequence of interbedded Plinian airfall deposits and ash-flow tuffs accompanying a large caldera subsidence and overlain by dacitic lavas. These tuffs provided K/Ar ages of 5.8±0.2 on biotite in dacitic clasts (Redwood and Macintyre, 1989) and 5.2±0.3 and 5.0±0.7 on two fractions of plagioclase from the crystal-rich ashy matrix (Bonhomme in Lavenu *et al.*, 1989). Unconsolidated ashy pyroclastic deposits contain abundant lithics and pumice blocks in a matrix which contains ~35% crystals of quartz, plagioclase and sanidine, biotite and small amounts of amphibole and magnetite. The stratigraphy of the Toba 76 tuff (that locally total 80 m thick) and the Perez ignimbrite (up to 50 m thick) are best observed along the rio Tirata (Fig. 4 A, Lavenu *et al.*, 1989). At the Estancia Chiriquiña where it is 15 to 30 m thick, the Toba 76 tuff (BO9, Fig. 4 B) lies directly above Miocene clays and sandstones (Crucero Formation) and is made up a complete eruptive episode. This single cooling unit consists of at least 3 distinct layers. The layer 1 is a thinly bedded Plinian ash and pumice fall deposit up to 2m thick. The layer 2 is a poorly sorted ash-fall deposit (0.20 to 2 m thick). The layer 3 is a salmon pink ash flow deposit with a biotite-rich base and minor amounts of lithics mixed with small pumices in a fine ashy matrix. The top of the flow unit is eroded in many places and consists of a reversely graded nonwelded coarse pumice-rich level with a fines-depleted matrix. Well-vesiculated crystal-rich rhyodacitic pumices contain dominant quartz, biotite and plagioclase with small amounts of amphibole and Fe-Ti oxides. The Toba 76 tuff and the Perez ignimbrite are separated by about 10–30 m of clastic sediments (Pliocene Umala Formation) at the Estancia Tirata. The Toba 76 tuff covers large areas of the western Cordillera, the central Altiplano and possibly the La Paz basin (Martinez, 1980). The Perez ignimbrite (BO7, Fig. 4 C) is more diverse vertically than the Toba 76 tuff. The depositional sequence is characterized by a typical plinian thinly bedded ash-fall deposit (3m thick) overlain by a thick (~1 m) surge layer with sandwave bed forms and two recognizable flow units. The 20m-thick lower flow deposit consists of a nonwelded fine-grained basal part, a poorly sorted pumices and lithics main body and a smaller upper part reversely graded with a coarse pumice-rich zone. A black-brown vitrophyre of 2 m thick is present at the base of the 20–30m-thick upper flow unit. This densely welded, typically light-gray-colored, pumice flow deposit exhibits columnar joints and coarse pumice concentrations are common, particularly at the top. The pumiceous matrix contains coarse pumices, lithics and quartz, biotite, plagioclase, amphibole, Fe-Ti oxides and rare small crystals of clinopyroxene. The Ayo Ayo tuff (LA82–2) is a single, non-welded, homogeneous, coloured, crystal-poor (~20%) flow deposit. The matrix is fine-grained with lithics and small dacitic pumices containing plagioclase, quartz, biotite, amphibole and Fe-Ti oxides.

A series of dacitic and rhyolitic tuffs is interbedded at different levels with the lacustrine or glacial formations of the La Paz and Titicaca basin (Lavenu, 1986, Lavenu *et al.*, 1989). The Chua tuff (La82–1), near lake Titicaca, is a coarse-grained, crystal-rich, densely welded, dacitic tuff showing numerous oxidized lenses. Crystals are dominantly quartz, biotite, plagioclase and small amounts of amphibole and Fe-Ti oxides. The Cota Cota tuff (MB161) from the lower part of the La Paz Formation, is a pale green-colored, fine-grained, welded deposit with rare mm-sized crystal fragments: plagioclase, biotite and amphibole in a devitrified glassy matrix. The Chijini tuff (PH54) from the upper part of the La Paz Formation, consists of a soft white rhyolitic deposit with sparse quartz and biotite in a very abundant ashy matrix. The Patapatani tuff (MB153) is also a white rhyolitic deposit which resembles the Chijini tuff and a correlation has been established (Lavenu *et al.*, 1989). The Purapurani tuff (PH53a) is a rhyolitic salmon-pink fall deposit with quartz, biotite, feldspar and glassy fragments.

GEOCHEMISTRY

Analytical Methods

The material analysed in this study consist of 23 fragments of vitrophyres, obsidians, pumices and glassy fractions of tuffs and fallout deposits from the Pacific piedmont and the western Cordillera in southern Peru, the Altiplano and the La Paz and Titicaca basin in northern

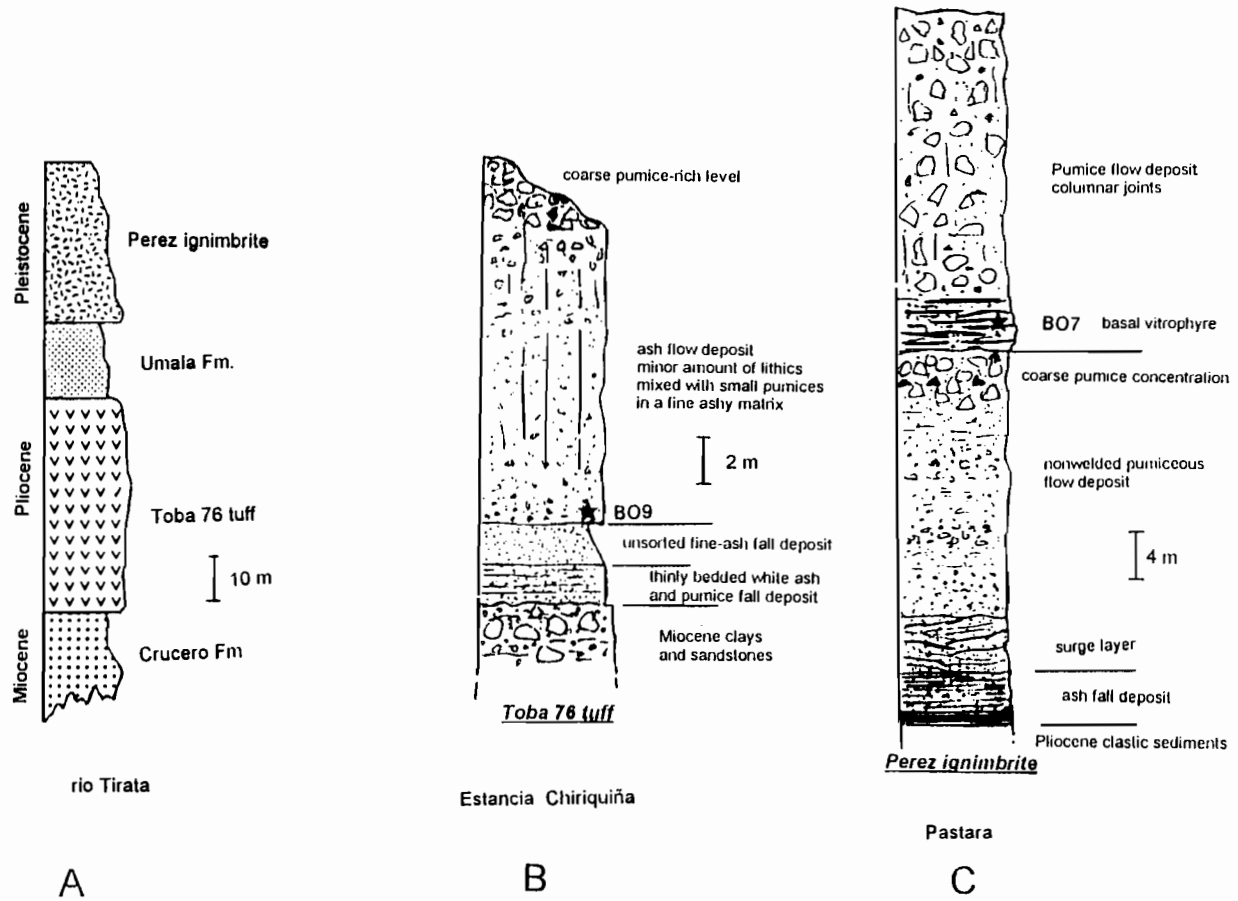

Fig. 4. Schematic stratigraphic colomns of the Toba 76 tuff and the Perez ignimbrite for two locations in the Tirata area. A: section at rio Tirata from Lavenu *et al.* (1989). B: section of the Toba 76 tuff at Estancia Chiriquiña. C: section of the Perez ignimbrite at Pastara.

Bolivia. In addition, 7 hydrated glasses from tuffs of the Bolivian Altiplano and the La Paz and Titicaca basin have also been analysed because their stratigraphic position is well-known (Table 1). Ulloma and Callapa tuffs are intercalated at different levels in the late Miocene sequences and are the only tuffs to be dated (Evernden *et al.*, 1977). Recent K/Ar dates have been obtained on the other tuffs (Ayo Ayo tuff and tuffs intercalated in La Paz Formation, Lavenu, 1986, Lavenu *et al.*, 1989). Nevertheless devitrification is a serious problem, therefore results on these tuffs are given for comparison. Samples were analysed for Zr, Nb, Y, Ba, Sr and Rb at the University Claude Bernard of Lyon using X ray fluorescence (XRF) method (Germanique and Briand, 1985). Rare earth elements (REE) plus Ta, Hf, Th, U, Sc and Cs contents were measured by instrumental neutron activation analysis (INAA) at the Institut Laüe-Langevin of Grenoble following the procedures of Oliver *et al.*, (1990). Geochemical data are presented in Table 4. Table 4 also includes SiO_2 and alkalies which have been recalculated to 100 wt% major element data on volatile-free basis. Seven samples with loss of ignition (LOI) > 3 wt% have not been excluded but are noted "hydrated glass" (HD) in Table 4. Other samples have between 0.5 and 3 wt% LOI. Major element compositions were determined on 6 glasses (Sa1,2,3–90, PH1–79c, 80–109, 80–104) by electron microprobe at the Centre Régional de Mesures Physiques of the University Blaise Pascal of Clermont-Ferrand and on other samples by energy dispersive X-ray fluorescence spectrometric method (EDXRF) at the University Joseph Fourier of Grenoble.

Geochemical Characteristics

Tuffs and associated fall deposits range in composition from high-silica rhyolite to andesite (78.8–57.6% SiO_2) and are subalkaline ($Na_2O + K_2O$ between 5.3–9.1, Table 4).

Representative minor and trace-element MORB-normalized patterns for tuffs from the four paleogeographic domains show differences which are illustrated by the multi-element diagram in Fig. 5. Plots of individual tuffs exhibit typical features for continental-margin volcanic arcs with marked enrichment mainly in the large ion lithophile (LIL) elements such as K, Rb, Ba and Th relative to the incompatible high-field strength (HFS) elements, notably Nb and Ta, and to all transitional elements. The LIL enrichment and HFS-depleted nature of Nb (and Ta geochemically similar to Nb) relative to Ce in subduction zones are well-known and generally attributed to a subduction component (McCulloch and Gamble, 1991; Smith and Leeman, 1993). Ce shows a same small positive anomaly for all samples. Nb and Ta show a distinct depletion which may be an indication that the source

Table 4 Trace-element compositions of obsidian fragments, pumices and glassy matrices of tuffs from southern Peru and northern Bolivia. SiO_2 and total alkali values correspond to major-element analyses recalculated to 100% on volatile-free basis.

	Peruvian Pacific piedmont							Peruvian western Cordillera							
N°	1	2	3	4	5	6	7	8	9	10	11	12	13	14	15
Sample	P-Pe3	P-Pe2	P-Pe53	P-Pe32	OF-SA1-90	OF-SA2-90	OF-SA3-90	G-Pe29	G-Pe17	P-Pe52	G-Pe44	P-Pe23	P-Pe33	BV-Pe42	BV-PH1-79
Trace element abundances															
Ba	720	616	434	928	993		952	586	828	497	936	496	806	520	
Rb	116	95	211	105	386			153	123	133	54	143	96	194	243
Sr	233	179	79	216	173			65	338	334	768	225	235	79	45
Y	14	15	17	14	19			18	19	16	16	18	16	15	
Zr	94	73	122	134	84		122	123	147	119	156	107	112	119	
Nb	10	11	13	11	14			10	10	8	9	12	11	12	
Sc	4.62	3.48	1.84	2.97	2.06	2.24	2.12	11.72	6.54	1.26	3.03	4.32	5.26	17.30	3.10
Hf	3.07	3.08	4.48	4.10	3.67	4.30	3.90	4.18	5.12	2.61	3.81	4.69	4.25	6.37	8.60
Ta	1.23	1.22	1.12	0.85	1.29	1.32	1.10	0.66	0.73	0.81	0.84	1.25	1.09	1.36	
Th	13.53	13.80	43.13	8.65	14.35	15.41	14.70	5.85	15.47	7.16	18.77	17.78	9.28	35.00	6.10
U	2.2	2.0	14.8	1.4	3.8	4.1	3.8	1.3	4.6	2.7	1.9	2.9	2.8	7.0	
Zr/Hf	30.7	23.6	27.1	32.7	22.9		31.3	29.4	28.8	45.4	41.0	22.8	26.3	18.6	
Th/Ta	11.0	11.3	38.5	10.2	11.1	11.7	13.4	8.9	21.2	8.8	22.3	14.2	8.5	25.7	
Sr/Y	16.5	12.2	4.5	15.5	9.1			3.6	17.5	20.6	48.9	12.4	14.6	5.2	
REE concentrations															
La	34.68	28.29	45.53	39.76	29.61	35.43	33.60	33.00	31.82	21.77	41.99	37.85	33.04	40.10	78.10
Ce	63.27	55.29	72.40	83.44	68.93	75.71	68.93	65.84	57.35	51.13	74.36	74.50	64.99	79.27	161.80
Nd	25.44	21.65	25.66	32.77	26.05	26.53	25.35	31.70	21.97	17.80	31.93	26.48	25.79	40.06	56.10
Sm	3.12	2.83	3.90	4.08	3.85	4.30	4.13	5.36	3.83	4.20	4.82	4.60	3.60	4.48	9.89
Eu	0.72	0.58	0.40	0.78	0.67	0.74	0.70	1.54	0.93	0.32	0.68	0.70	0.85	1.92	0.76
Gd	3.72	3.26	4.11	3.90	5.11	5.75	4.84	4.83	3.66	4.05	5.08	5.06	3.78	4.23	8.31
Tb	0.70	0.60	0.72	0.64	1.01	1.14	0.90	0.76	0.60	0.67	0.89	0.91	0.66	0.69	1.23
Yb	1.86	1.48	1.47	1.61	1.31	1.46	1.45	1.20	1.47	1.45	1.96	2.04	2.23	1.67	2.80
Lu	0.32	0.22	0.19	0.21	0.20	0.20	0.19	0.19	0.21	0.23	0.32	0.30	0.30	0.26	0.38
SREE	133.83	114.20	154.38	167.19	136.74	151.26	140.09	144.42	121.84	101.62	162.03	152.44	135.24	172.68	319.37
La/Yb(N)	12.47	12.78	20.71	16.51	15.11	16.23	15.50	18.39	14.47	10.04	14.33	12.41	9.91	16.06	18.65
La/Sm(N)	6.86	6.17	7.20	6.01	4.75	5.08	5.02	3.80	5.13	3.20	5.38	5.08	5.66	5.52	4.87
Ce/Yb(N)	8.65	9.50	12.53	13.18	13.38	13.19	12.09	13.95	9.92	8.97	9.65	9.29	7.41	12.07	14.70
major elements recalculated to 100 wt% on a volatile-free basis															
SiO2	72.7	72.8	74.7	73.6	75.5	76.4	76.5	73.5	67.2	65.6	61.3	70.7	72.9	75.9	74.7
Na2O	4.19	3.67	3.37	4.57	4.57	3.64	3.85	3.88	4.10	2.75	4.15	4.35	3.75	4.00	2.83
K2O	4.25	4.99	5.10	3.97	4.51	4.62	4.54	4.98	3.58	3.03	2.39	3.93	3.70	4.92	5.56
Na2O+K2O	8.44	8.66	8.47	8.54	9.08	8.26	8.39	8.86	7.68	5.78	6.54	8.28	7.45	8.92	8.39
K/Rb	303	436	200	313	97			269	242	189	367	227	321	210	190

sample number prefixes are as follows: BV, basal vitrophyre, F, fiamme, HG, hydrated glass, G, glass, OF, obsidian fragment, P, pumice. Sample locations and ages are indicated in Table 1.

Table 4 Continued

	Peruvian western Cordillera (cntd)				Bolivian Altiplano						La Paz and Titicaca basin				
N°	16	17	18	19	20	21	22	23	24	25	26	27	28	29	30
Sample	F-80-109	F-80-104	P-Pe18	F-Pe8	HG-PH64	HG-PH61	G-PH48	P-BO9	BV-BO7	HG-LA82-2	G-LA82-1	HG-MB161	HG-PH54	HG-MB153	HG-PH53a
Trace element abundances															
Ba		1038	838	760	608	540	1101	863	721	719	1035	467	388	639	918
Rb	7	104	98	76	114	244	158	124	103	103	136	118	127	126	102
Sr	256	65	565	626	225	246	487	516	338	312	684	295	209	371	427
Y			15	17	11	20	18	14	10	13	23	7	12	13	13
Zr			128	164	107	183	199	116	152	155	190	119	129	127	134
Nb			9	8	13	15	16	17	13	13	21	11	14	13	12
Sc	1.°0	4.10	8.54	15.27	3.60	5.37	7.21	3.78	2.65	2.34	10.80	1.96	1.65	1.93	2.41
Hf	2.80	9.83	4.51	5.00	3.67	6.21	6.12	4.13	4.53	4.77	6.13	3.53	3.96	4.17	4.99
Ta		1.15	0.86	0.68	1.35	2.58	1.17	1.22	1.40	1.04	2.27	0.68	1.29	1.25	0.91
Th	1.30	13.58	13.68	9.92	16.89	18.97	16.28	15.19	12.40	14.57	13.42	15.59	14.23	11.66	12.85
U		2.6	3.4	2.6	4.4	10.6	3.5	4.6	3.5	3.8	3.0	4.4	4.2	3.6	2.8
Zr/Hf			28.4	32.7	29.1	29.4	32.5	28.1	33.6	32.4	30.9	33.8	32.6	30.4	26.8
Th/Ta		11.8	15.9	14.6	12.5	7.4	13.9	12.5	8.9	14.0	5.9	22.9	11.0	9.3	14.1
Sr/Y			38.1	37.9	20.3	12.2	27.2	37.4	34.2	24.0	30.3	44.7	17.2	29.2	32.6
REE concentrations															
La	25.20	42.93	33.30	29.77	39.67	63.88	59.93	37.66	54.91	45.90	54.36	27.98	47.69	46.57	55.18
Ce	49.70	96.18	65.71	66.24	67.42	138.19	114.60	59.39	92.13	81.19	108.52	41.46	90.41	90.07	105.07
Nd	16.40	45.56	25.82	29.58	20.64	57.41	46.31	20.02	28.41	26.74	40.41	11.39	27.16	27.33	30.73
Sm	2.80	6.86	4.63	5.05	3.39	10.18	7.63	3.50	4.18	4.01	7.36	1.99	4.08	3.94	4.31
Eu	0.53	1.58	1.19	1.42	0.81	1.44	1.66	0.94	1.02	0.91	1.81	0.42	0.71	0.98	1.20
Gd	2.04	6.78	4.72	4.99	3.87	8.64	5.42	2.25	2.66	2.48	7.05	1.72	4.04	3.91	4.24
Tb	0.26	1.14	0.81	0.84	0.71	1.29	0.67	0.24	0.28	0.28	1.16	0.26	0.68	0.66	0.71
Yb	1.00	2.71	1.49	1.60	1.22	1.73	1.53	0.90	1.03	1.16	2.14	0.61	0.98	1.08	1.00
Lu	0.14	0.36	0.21	0.25	0.22	0.26	0.22	0.14	0.15	0.17	0.31	0.08	0.14	0.14	0.15
SREE	98.07	204.10	137.88	139.74	137.95	283.02	237.97	125.04	184.77	162.84	223.12	85.91	175.89	174.68	202.59
La/Yb(N)	16.85	10.59	14.94	12.44	21.74	24.69	26.19	27.98	35.65	26.46	16.99	30.67	32.54	28.83	36.90
La/Sm(N)	5.55	3.86	4.44	3.64	7.22	3.87	4.85	6.64	8.11	7.06	4.56	8.68	7.21	7.29	7.90
Ce/Yb(N)	12.64	9.03	11.22	10.53	14.00	20.32	19.05	16.78	22.75	17.80	12.90	17.29	23.46	21.21	26.72
major elements recalculated to 100 wt% on a volatile-free basis															
SiO2	78.8	73.5	61.6	57.6	73.3	70.7	64.9	70.4	74.3	72.8	66.1	66.3	74.2	74.5	75.0
Na2O	1.66	2.77	3.89	3.76	5.08	4.63	2.70	3.69	3.77	2.63	3.56	3.73	3.32	3.33	3.36
K2O	3.67	5.59	2.43	2.24	2.31	2.82	3.96	4.12	4.54	5.76	3.47	4.00	5.25	5.42	5.59
Na2O+K2	5.33	8.36	6.32	6.00	7.39	7.45	6.66	7.81	8.31	8.39	7.03	7.73	8.57	8.75	8.95
K/Rb	170	446	206	244	168	96	209	275	367	463	211	282	343	356	453

sample number prefixes are as follows: BV, basal vitrophyre, F, fiamme, HG, hydrated glass, G, glass, OF, obsidian fragment, P, pumice. Sample locations and ages are indicated in Table 1.

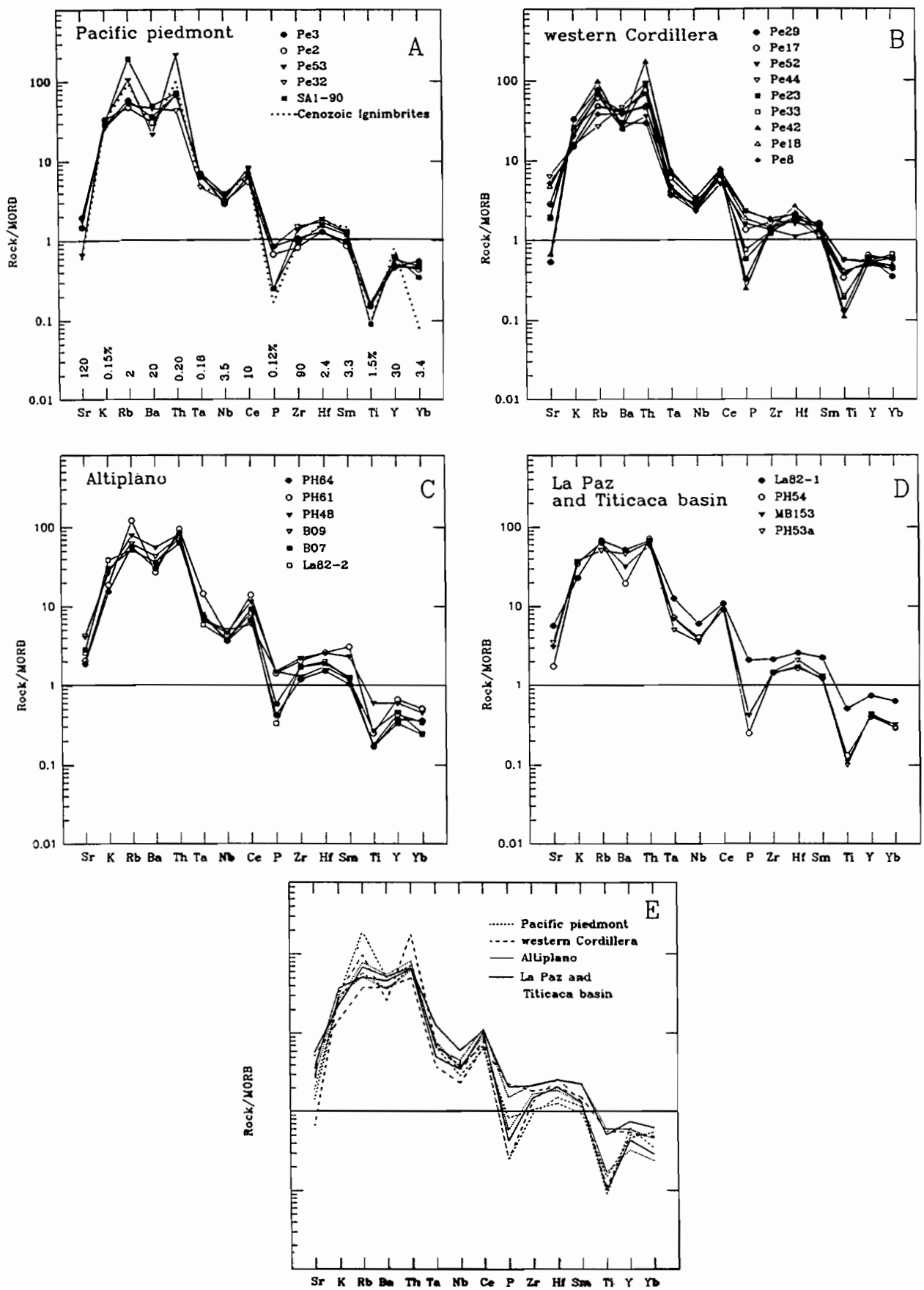

Fig. 5. MORB-normalized multi-element variation diagram for selected tuffs from A: the Pacific piedmont, B: the western Cordillera, C: the Altipolano and D: the La Paz and Titicaca basin. E: comparison of trace element distributions for samples respectively the most evolved and least evolved compositions of each group. Normalizing factors shown on X axis of A taken from Pearce (1983). Cenozoic ignimbrites from Schmitt-Riegraf and Pichler (1988).

of at least some of the magma is of mantle origin. The trace element patterns of these tuffs are very similar to those of Cenozoic ignimbrites plotted in Fig. 5A (Schmitt-Reigraf and Pichler, 1988). Compositional differences between the obsidian glass (SA1–90) and the pumices (Pe32) of the SA tuff are small depletions of Rb and Ba in the pumice with respect to the glass, other elements as Hf and Ta having broadly similar concentrations. The relative Sr enrichment for andesitic and dacitic tuffs from the western Cordillera (Fig. 5B) indicate plagioclase control and is coherent with subduction-related magmas (Luhr, 1992). The anomaly of Ba may be an indication of refractive mineral phases, possibly phlogopite and amphibole, in the source or the fractionation of the plagioclase. Decreases of Zr from dacites to rhyolites may be interpreted as the fractionation of biotite (Davidson *et al.*, 1990). Positive anomalies for Rb and Th relative to Ba and negative anomalies for Sr, P and Ti increase from dacitic tuffs to high-silica rhyolitic tuffs (Fig. 5B and C). Some obsidian glasses and homogeneous vitrophyres (SA1–90, Pe42) are distinguished by their higher abundances of Rb and Th relative to pumices and glass matrices. Strong negative anomalies of Sr, P and Ti are very typical for arc magmas (Pearce, 1983) and reflect the importance of plagioclase, apatite, ilmenite or Ti-magnetite in the fractionating assemblage of these tuffs, independently of their age and their position from the trench. Trace element compositions of hydrothermally altered tuff deposits from the Altiplano and the La Paz and Titicaca basin (Fig. 5D and E) approach those found in nonaltered tuffs from the western Cordillera and the Pacific piedmont and in some cases are indistinguishable except for the Cota Cota tuff (MB161, not shown in Fig. 5D). We conclude that in these cases, the compositions of tuffs in minor and trace elements are relatively little affected by post-magmatic hydrothermal alteration.

Among all incompatible elements, Zr and Hf are especially interesting elements with respect to their excellent concentration in late forming mineral as ilmenite. Figure 6 is a plot of Zr vs Hf for all the tuffs and highlight some differences in Zr and Hf contents. The abundances of Zr and Hf are generally greater in tuffs of the Altiplano than those of the western Cordillera at comparable SiO_2 contents. Zr/Hf values range from 18 to 45 with the majority of values varying between 25–35, as commonly observed in rhyolites (Hildreth and Moorbath, 1988). The mean Zr/Hf ratio is 27 for the rhyolitic tuffs of the Pacific piedmont and the western Cordillera and 30 for the rhyolitic tuffs of the Altiplano and La Paz and Titicaca basin. This last value is close to the value of 30.4 for the northern Chilean ignimbrites (de Silva and Francis, 1989; Davidson *et al.*, 1990). However, Hf contents are more scattered in tuffs from the western Cordillera and the Zr/Hf ratios vary from 18 for a high-silica vitrophyre (Pe42) to 41 and 45 for two dacitic tuffs (Pe44 and Pe52): values which are also found in other pyroclastics in the CVZ (de Silva et al., 1993).

Figure 7 illustrates the range of Ta and Th contents of the majority of tuffs, with the exception of four samples

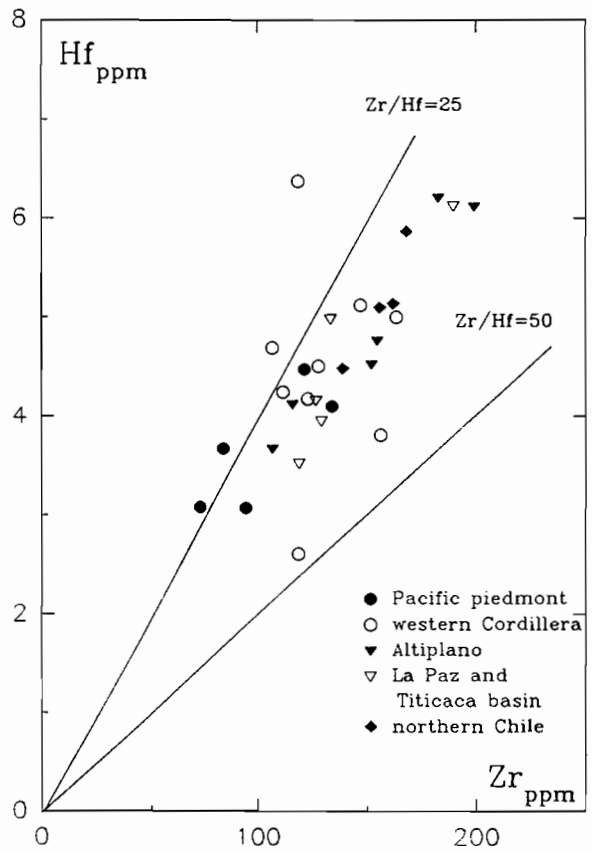

Fig. 6. Hf-Zr correlation diagram for selected tuffs from southern Peru and northern Bolivia. Ignimbrites of northern Chile taken from de Silva and Francis (1989) and Davidson *et al.* (1990).

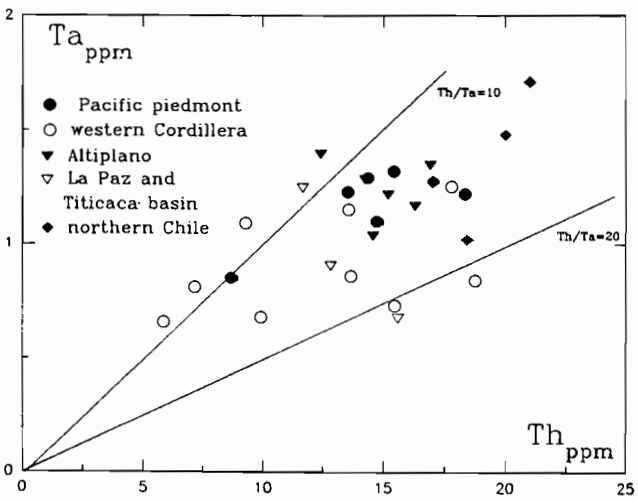

Fig. 7. Th-Ta diagram for selected tuffs from southern Peru and northern Bolivia. Ignimbrites of northern Chile as in Fig. 6.

which have anomalously high Th or Ta contents and plot just outside this field. For the other tuffs, Th and Ta contents are compared with those from northern Chile. Th/Ta ratios are high and variable and range from 7 to 15 in rhyolites with a mean value of 11 for all groups. This value is close to 10 which is a typical value for continental arc magmas. Other samples plot in the same area as ignimbrites from the CVZ (Davidson *et al.*, 1990) and

close to the Th/Ta value of 20, reflecting a strong crustal influence.

Rare Earth Elements

Chondrite-normalized REE distribution patterns for all tuffs (Table 4, Fig. 8) show moderate to high REE contents (98–319) with the exception of the Cota Cota tuff (MB161) which have unusually low REE contents (~86) and fractionated patterns. Relations are similar to those of high-K calc-alkaline ash-flow tuffs in convergent margins with large light REE concentrations and light/heavy REE (LREE/HREE) ratios. These tuffs are enriched in LREE (60–180 times chondritic abundances) with La/Yb_N varying from 10 to 36 (between 10–20 for tuffs from the Pacific piedmont and the western Cordillera and between 15–36 for those from the Bolivian Altiplano and the La Paz and Titicaca basin). Abundances of the LREEs are well correlated with those of other incompatible elements such as Ba, Zr and P (*e.g.* for the tuffs from the Bolivian Altiplano: PH48 and La82–1 or from the western Cordillera: Pe44). The highest total REE contents (>200 ppm) correspond to the higher Y values (>20 ppm, *e.g.* the Chua tuff LA82–1). As reported by Cameron and Hanson (1982) and Wark (1991), Y behaves similar to a HREE and its variations are consistent with the decreasing importance of hornblende fractionation.

Rhyolitic tuffs of the Pacific piedmont (Fig. 8A) show moderate LREE enrichments, depleted HREEs and pronounced negative Eu anomalies. Their distribution patterns are parallel but slightly depleted to other CVZ ignimbrites (Schmitt-Riegraf and Pichler, 1988). The REEs of obsidian glasses and pumices of the SA tuff

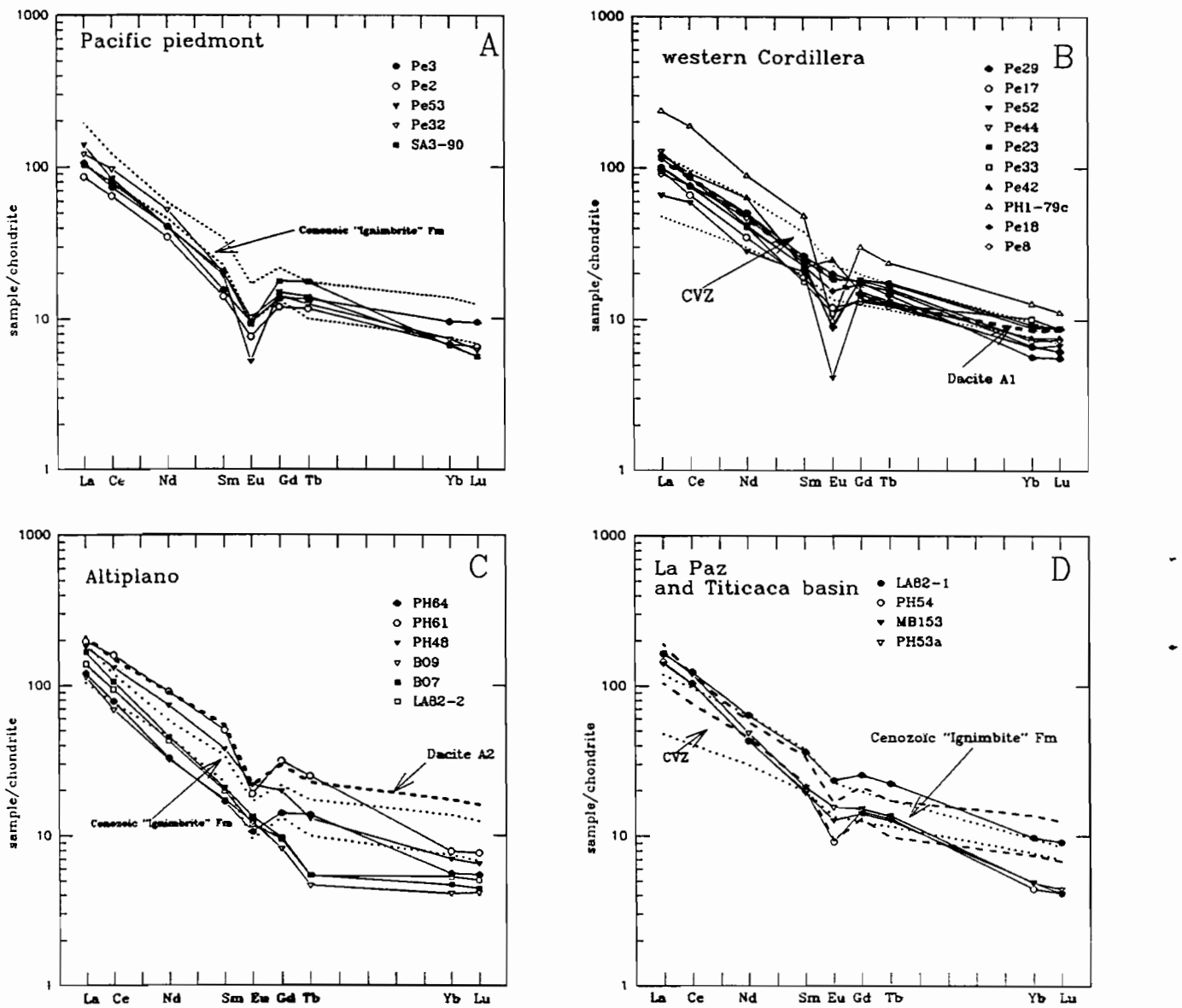

Fig. 8. Chondrite-normalized REE abundances for tuffs from A: the Pacific piedmont, B: the western Cordillera, C: the Altiplano and D: the La Paz and Titicaca basin. Normalizing values after Nakamura (1974). "Ignimbrite" field of Central Andes from Schmitt-Riegraf and Pichler (1988). CVZ field from Thrope *et al.* (1984). Dacite A1 and Dacite A2 from Lefévre (1979).

(SA3–90) exhibit similar patterns of typical calc-alkaline high-silica rhyolite and show enrichment in the LREEs relative to the HREEs (La/Yb_N = 15–16). From light to heavy elements, concentrations decrease from about 100 times for La to about 5 to 8 times chondritic abundances for Yb. Compared to the basal vitrophyre of the Cotahuasi tuffs (PH1–79c, Fig. 8B) in the western Cordillera having similar SiO_2 contents, typical glasses of the SA tuff are relatively less enriched in LREEs (La = 90–108 times chondrites) than the Cotahuasi vitrophyre (up to 200 times for La). This vitrophyre with the highest REE contents show a larger negative Eu anomaly similar to this of another tuffs of the Pacific piedmont (Pe53).

Tuffs of intermediate to dacitic compositions of the western Cordillera (Fig. 8B) display typical characteristics of the CVZ. They have nearly linear trends but slightly depleted in HREEs (La/Yb_N = 10–14) and exhibit a weak Eu anomaly that might indicate major plagioclase fractionation. The more evolved rhyolitic tuffs and obsidians display moderate to pronounced negative Eu anomalies (*e.g.* Pe52 and PH1–79c) which suggests extensive plagioclase fractionation except for one rhyolitic vitrophyre (Pe42) characterized by a small positive Eu anomaly inside the precision of the analytical technique. Similar REE patterns in dacites are also found in many other calc-alkaline Cenozoic andesite-rhyolite associations. The REE distribution patterns of these dacitic tuffs is parallel to the Dacite A1 trend defined by Lefévre (1979) for dacites of southern Peru and reported to the Cenozoïc volcanic activity between 150–250 km from the Peru-Chile trench.

More important for later discussions are the observation that dacitic tuffs of the Altiplano (Fig. 8C) are compositionally distinct. The REE patterns for three Bolivian tuffs (the Toba 76 tuff, the ignimbrite Perez and the Ayo Ayo tuff) differ from the others and are weakly concave upward (115–165 times chondrites for La) and flat for HREEs (about 5 times chondrites). This could be due to source differences given that the Bolivian tuffs are from ~350–400 kms further from the Peru-Chile trench. None of these rhyolitic tuffs exhibit Eu anomalies, which would confirm that either little plagioclase was extracted during crystallization. Miocene tuffs of the Bolivian Altiplano which display little evidence of alteration with LOI > 3 wt.%, exhibit distribution patterns similar for light and middle REE to the Dacite A2 trend reported by Lefévre (1979) to Cenozoic volcanic activity between 250–400 km from the Peru-Chile trench. REE distribution pattern of the Ulloma tuff (PH64) is parallel but slightly depleted relative to this of the Callapa tuff (PH61). These samples show no evidence for any negative Ce anomalies resulting from incipient alteration due to weathering in volcanic rocks (Price *et al.*, 1991). The Callapa tuff (PH61) has high Ce and lower HREE contents that yields a high Ce/Yb_N ratio of 20. It is concluded that the weathering of these tuffs is without influence on their REE distribution patterns.

Tuffs of the La Paz and Titicac basin are strongly LREE enriched and HREE depleted as other Bolivian tuffs (Fig. 8D). These tuffs interbbeded with lacustrine formations show almost identical and parallel REE patterns with minor Eu anomalies for the Chua and Chijini tuffs. REE pattern of the Chijini tuff closely resemble those of Miocene tuffs. Three Plio-Pleistocene tuffs display LOI > 3 wt%, but have high Ce abundances and the highest Ce/Yb_N ratios (21–27), therefore their alteration is considered, as for the Miocene tuffs, without influence on their REE distribution patterns.

DISCUSSION AND CONCLUSIONS

Ages of tuffs and plinian fall deposits from southern Peru and northern Bolivia between 15°S and 18°S are well-established and new geochemical data of these tuffs permit to compare trace-element and REE contents for dacite-rhyolite tuffs from the western Cordillera and its piedmont to those from the northern Bolivian Altiplano and the eastern Cordillera piedmont. As a starting point for discussion, we emphazise that geochemical variations of these tuffs may be a consequence of the tectonic complexity in these areas and may provide evidence of the heterogeneity of the magma source regions. Most authors agree on a crustal thickness slightly more than 50 km beneath the Bolivian Altiplano and a 30° east dipping angle of the subducted slab between 17°S and 20°S. Cahill and Isacks (1992) argued that the presence of an asthenospheric wedge overlying the subducting Nazca plate is presumed to govern the process of magma generation. Dorbath *et al.*, (1993) predicted that the subduction of young oceanic lithosphere at a high speed for a substantial time could produce hot mantle under the Altiplano and evidenced a major suture at the eastern border of the La Paz and Titicaca basin (eastern Cordillera piedmont). In southern Peruvian and northern Bolivian Andes, unconformities are overlain by tuffs and only in some cases these tuffs are slightly folded and faulted (*e.g.* the Toba 76 tuff and the Chijini tuff in northern Bolivia). This explosive volcanism may be interpreted in response to upper-crustal shortening and thickening during Quechua compressional events at ~25, ~17, ~10, ~7 and ~2.5 Ma (Lavenu, 1986; Sébrier *et al.*, 1988; Mercier *et al.*, 1992) During Miocene times (7–8 Ma), a major compressional deformation induced a strong NE-SW shortening in the High Andes of Bolivia (northern Altiplano and eastern Cordillera, Lavenu and Mercier, 1991). This tectonic event could be the paroxismal expression of a compressional period which affected the Andean Chain during the late Oligocene-Miocene times (Baby *et al.*, 1990; Sempéré *et al.*, 1990, 1991). The orogenic structuration of the Bolivian Altiplano and the western part of the eastern Cordillera has been acquired through thrusts and strike-slip faults during this period (Hérail *et al.*, 1993) and the Andean Chain reached its present topographical evolution at this time. Thickening of the crust during uppermost Miocene (~7 Ma) and upper Pliocene (~2.5 Ma) compressional pulses was directly associated with uplift of the High Andes in Peru and Bolivia (Sébrier *et al.*, 1988). Crustal shortening after 10 Ma have played an important role in controlling the magmatic processes initiated by

subduction. Tuffs took place at successive extensional periods during which thermal weakening and thinning of the crust related to lengthening and increase in dip of the slab probably occurred (Mercier *et al.*, 1992). Voluminous peraluminous ash-flow tuffs in the Morococala and Los Frailes volcanic fields (Ericksen *et al.*, 1990) are of late Miocene age (Morococala tuffs, 6.3–5.8 Ma; Lavenu, 1986 and Los Frailes tuffs, 8.5–6.4 Ma; Koeppen *et al.*, 1987). These geophysical and tectonic data suggest that changes in tectonic regimes of the southern western Cordillera and northern Bolivian Altiplano which occured with each Quechua tectonic pulse and which affected the astenospheric wedge and both the dowgoing and the overriding lithospheres may be responsible for the trace element diversity observed in tuffs along the east-west traverse from the Pacific piedmont in Peru to the eastern Cordillera piedmont in Bolivia.

With the exception of vitrophyres from the Cotahuasi region in the western Cordillera and the Cota Cota tuff of the La Paz and Titicaca basin, the incipient hydratation observed in glasses of some tuffs and due to weathering might have relatively no influence on their REEs and other trace element concentrations. These concentrations, similar to those of nonaltered tuffs, may be considered to reflect the magmatic processes and compositions of tuffs. Trace-element compositions and REE concentrations in tuffs correspond closely with the composition of the lava flows for a given whole-rock SiO_2 content. Tuffs have trace element signature typical of subduction-related continental arc magmatism, showing a strong LILE/HFSE enrichment and nonenrichment of HREE and Y, as pointed out by Gill (1981). It is difficult to evaluate the effects of fractionation and assimilaltion in these tuffs which exhibit a restricted range in SiO_2 (the majority have 61–76%SiO_2). However, some space-related observations can be made on the basis of their geochemical characteristics and differences in age. During Neogene-Pleistocene times it appears two distinct groups of tuffs. Tuffs erupted in northern Bolivia are typically enriched in Zr, Hf, Th and LREEs relative to those erupted in southern Peru, at a given SiO_2 content (65–67 wt.% for dacites and 72–73 wt.% for rhyolites). These two types of enrichments may be related to differences in subduction processes and could be consistent with their derivation from different magma sources. The higher values in Bolivian tuffs suggest an enriched mantle source. Ratios of Ce/Yb_N increase eastward from 7–13 (mean value of 11) for Peruvian tuffs to 13–27 (mean value of 19) for Bolivian tuffs, values which could indicate variable degrees of melting of mantle source. Along the Central American arc, such variations are linked to the subduction geometry and volume of the astenospheric wedge (Carr *et al.*, 1990). In the case of Neogene and Pleistocene tuffs of southern Peru and northern Bolivia, higher Ce/Yb_N ratios could reflect the variation of degree of wedge contribution toward the east. The late Miocene to Pliocene Bolivian tuffs have high Th/Ta ratios (10–15), high Th/Nb ratios close to those of other CVZ tuffs (de Silva and Francis, 1989) and high Nd contents (20–46 ppm). As shown by Hawkesworth and Clarke (1994), the high Nd values could reflect magma differentiation processes, perhaps associated with crustal contamination, smaller degrees of partial melting and/or higher trace element abundances in the source. Highly fractionated REE patterns of Bolivian tuffs may be attributed to intensive crustal contamination. These results are consistent with the interpretation of isotopic variations of Quaternary volcanics in Central Andes between 17°S and 22°S which allow Wörner *et al*, (1992) and Davidson and de Silva (1992) to provide evidence for major crustal contribution to arc magma genesis, surimposed on variations in the mantle source composition.

Especially after the upper Miocene compressional phase which was a time of major crustal growth in the CVZ, tuffs erupted between 5 and 2.8 Ma have much lower Sr/Y ratios (4.5–15.5) in southern Peru than those erupted in northern Bolivia (24–37.5). These differences in tuffs of the same age erupted at 150–250 km or 250–400 km from the Peru-Chile trench may be interpreted as reflecting variable contributions from the mantle wedge and partial melting of the subducted lithosphere. The Bolivian tuffs have a large degree of LREE enrichement relative to HREE and high Ce/Y ratios. These data provide additional evidence for the importance of the compressional event at ~7 Ma and support our interpretation that these differences in magma chemistry may be attributed to the subduction of a warm oceanic lithosphere under the Bolivian Altiplano (Dorbath *et al.*, 1993). Such a phenomenon might have led to partial melting of the subducted lithosphere rather than of the mantle wedge (de Boer *et al.*, 1991)

FT dating of obsidian glass fragments of the SA Tuff have yielded an age of ***2.42±0.11 Ma*** similar in age to the Vitor tuff at 2.76±0.10 Ma. The SA tuff is not contemporaneous with the Toba 76 tuff or the Perez ignimbrite from the Bolivian Altiplano as it has been proposed. These tuffs typically date the last Quechua compressional phase during the lower Pleistocene (ca. 2.5 Ma) and the characteristics of magmas erupted before and after this phase essentially remained the same. Geochemical data record the effects of changes in the subduction beneath the southern Peru and northern Bolivia during the late Miocene compressional events. This would appear to confirm that from the last compressional event, the geodynamical situation remained one of high convergence. Geochemical data of Bolivian tuffs yielding an age between 5 and 2.8 Ma provide evidence that the upper Miocene (~7 Ma) compressional deformations were a major event prior to these tuff emplacements and played the most important role on the variability of the geochemical characteristics of the southern Peruvian and northern Bolivian tuffs.

Acknowledgements — This work is part of a continuing program on the dating and characterization of Peruvian Neogene silicic tuffs. Two of us (G.P. and N.V.-P.) thank "Multiciencias", Lima, for partial support in field work in Peru. G. Poupeau is indebted to Dr. Victor Latorre, "Multiciencias" Director, and the International Center for Theoretical Physics (Trieste) for pluri-annual support in Peru. We are grateful to the Institut

Français de Recherche Scientifique pour le Développement en Coopération (ORSTOM) for his logistical support and assistance during fieldwork in Bolivia, Christian Picard for a critical reading of an earlier draft and C.W. Naeser and S. de Silva for thorough, constructive reviews which resulted in substantial improvement of this paper. This paper is a contribution to I.G.C.P. project 345 "Lithospheric evolution of the Andes".

REFERENCES

Baby, P., Sempéré, T., Oller, J., Barrios, L., Hérail, G. and Marocco, R., 1990. Un bassin en compression d'âge Oligo-Miocéne dans le sud de l'Altiplano bolivien. *Compte Rendus de l'Académie des Sciences, Paris,* **311**, 341–347.

Bellon, H. and Lefévre, C., 1976. Données géochronologiques sur le volcanisme andin dans le sud du Pérou. Implications volcanotectoniques. *Compte Rendus de l'Académie des Sciences, Paris,* **283**, 1–4.

Bigazzi, G., Dompnier, E., Hadler Neto, J.C., Poupeau, G. and Vuilliez, E., 1988. A reactor rule calibration for fission-track dating and Uranium micromapping. *Nuclear Tracks Radiation Measurement,* **15**, 755–757.

de Boer, J.Z., Defant, M.J., Stewart, R.H. and Bellon, H., 1991. Evidence for active subduction below western Panama. *Geology,* **19**, 649–652.

Cahill, T. and Isacks, B.L., 1992. Seismicity and shape of the subducted Nazca plate. *Journal of Geophysical Research,* **97**, 17503–17529.

Cameron, K.L. and Hanson, G.N., 1982. Rare Earth element evidence concerning the origin of voluminous mid-Tertiary rhyolitic ignimbrites and related volcanic rocks, Sierra madre Occidental, Chihuahua, Mexico. *Geochimica et Cosmochimica Acta,* **46**, 1489–1503.

Carr, M.J., Feigenson, M.D. and Bennett, E.A., 1990. Incompatible element and isotopic evidence for tectonic control of source mixing and melt extraction along the Central American arc. *Contributions to Mineralogy and Petrology,* **105**, 369–380.

Davidson, J.P., McMillan, N.J., Moorbath, S., Wörner, G., Harmon, R.S. and Lopez-Escobar, L., 1990. The Nevados de Payachata volcanic region (18°S/69°W, N. Chile) II. Evidence for widespread crustal involvement in Andean magmatism. *Contributions to Mineralogy and Petrology,* **105**, 412–432.

Davidson, J.P. and de Silva, S.L., 1992. Volcanic rocks from the Bolivian Altiplano: insights into crustal structure, contamination and magma genesis in the Central Andes. *Geology,* **20**, 1127–1130.

Dorbath, C., Granet, M., Poupinet, G. and Martinez, C., 1993. A teleseismic study of the Altiplano and the Eastern Cordillera in northern Bolivia: new constraints on a lithospheric model. *Journal of Geophysical Research,* **98**, 9825–9844.

Dorighel, O., Poupeau, G., Bouchard, J.-F. and Labrin, E., 1994. Datation par traces de fission et étude de provenance d'artefacts en obsidienne des sites archéologiques de La Tolita (Equateur) et Inguapi (Colombie). *Bulletin de la Société de Préhistoire de France,* in press.

Ericksen, G.E., Luedke, R.G., Smith, R.L., Koeppen, R.P. and Urquidi F., 1990. Peraluminous igneous rocks of the Bolivian tin belt. *Episodes,* **13**, 1–7.

Evernden, J.F., Kriz, S.J. and Cherroni M, C., 1966. Correlaciones de las formaciones terciarias de la cuenca altiplanica a base de edades absolutas determinadas por el metodo Potasio-Argon. *Servicio Geologíco de Bolivia,* Hoja inf. n° 1.

Evernden, J.F., Kriz, S.J. and Cherroni M, C., 1977. Potassium-Argon ages of some Bolivian rocks. *Economic Geology,* **72**, 1042–1061.

Fenner, C.N., 1948. Incandescent tuff flows in southern Peru. *Bulletin of the Geological Society of America,* **59**, 879–893.

Francis, P.W. and Hawkesworth, C.J., 1994. Late Cenozoic rates of magmatic activity in the Central Andes and their relationships to continental crust formation and thickening. *Journal of the Geological Society, London,* **151**, 845–854.

Germanique, J.C. and Briand B., 1985. XRF determination of Zr, Nb, Y, Sr, Rb, Zn and Pb in fifteen International geochemical reference samples. *Geostandards Newsletters,* **9**, 31–34.

Gill, J.B., 1981. *Orogenic andesites and Plate tectonics.* Springer Verlag, Berlin, 310 p.

Gleadow, A.J.W., 1981. Fission track dating methods: what are the real alternatives? *Nuclear Tracks,* **5**, 3–14.

Grange, F., Cunningham, P., Gagnepain, J., Hatzfeld, D., Molnar, P., Ocola, L., Rodrigues, A.L., Roecker, S.W., Stock, J.M. and Suarez, G., 1984. The configuration of the seismic zone and the downgoing slab in southern Peru. *Geophysical Research letters,* **11**, 38–41.

Hawkesworth, C.J. and Clarke, C.B., 1994. Partial melting in the lower crust: new constraints on crustal contamination processes in the central Andes. In: *Tectonics of the Southern Central Andes* (edited by K.-J Reutter, E. Scheuber and P.J. Wigger), pp. 93–101. Springer-Verlag, Heidelberg, Germany.

Hérail, G., Soler, P., Bonhomme, M. et Lizeca, J.L., 1993. Evolution géodynamique de la transition entre l'Altiplano et la Cordillére Orientale au nord d'Oruro (Bolivie). Implications sur le déroulement de l'orogenése andine. *Compte Rendus de l'Académie des Sciences, Paris,* **317**, 515–522.

Hildreth, W. and Moorbath, S., 1988. Crustal contributions to arc magmatism in the Andes of Central Chile. *Contributions to Mineralogy and Petrology,* **98**, 455–489.

Hurford, A.J., 1990. International Union of Geological Sciences, subcommission on Geochronology recommandation for the standardization of fission track dating calibration and data reporting. *Nuclear Tracks Radiation Measurement,* **17**, 233–236.

Hurford, A.J. and Green, P.F., 1983. The zeta age calibration of fission-track dating. *Isotope Geosciences,* **1**, 285–317.

Isacks, B.L., 1988. Uplift of the Central Andean plateau and bending of the Bolivian orocline. *Journal of Geophysical Research,* **93**, 3211–3231.

Jenks, W.F. and Goldich, S.X., 1956. Rhyolitic tuff flows in southern Peru. *Journal of Geology,* **64**, 156–172.

Koeppen, R.P., Smith, R.L., Kunk, M.J., Flores, A., Luedke, R.G. and Sutter, J.F., 1987. The Morococala volcanics: highly peraluminous rhyolite ash flow magmatism in the Cordillera Oriental, Bolivia (abs.). *Geological Society of America Abstracts with Programs,* **19**, 731.

Laharie, R. and Derruau, M., 1974. La morphogenése des Andes du Sud du Pérou. *Revue de Géographie Alpine,* **70**, 479–505.

Lavenu, A., 1986. *Etude néotectonique de l'Altiplano et de la Cordillére orientale des Andes Boliviennes.* Unpublished Thesis, University of Paris-Sud, Orsay, 434 p.

Lavenu, A., Bonhomme, M.G., Vatin-Pérignon, N. and De Pachtére, P., 1989. Neogene magmatism in the Bolivian Andes between 16°S and 18°S: stratigraphy and K/Ar geochronology. *Journal of South America Earth Sciences,* **2**, 35–47.

Lavenu, A. et Mercier, J.-L., 1991. Evolution du régime tectonique de l'Altiplano et de la Cordillére Orientale des Ande de Bolivie du Miocéne supérieur à l'Actuel. Un effet des forces de gravité et des forces aux limites. *Géodynamique,* **6**, 21–55.

Lefévre, C., 1979. *Un exemple de volcanisme de marge active dans les Andes du Pérou (Sud) du Miocéne à l'Actuel (Zonations et pétrogenése des andésites et des shoshonites).* Unpublished Thesis, University of Montpellier, 555 p.

Luhr, J.F., 1992. Slab-derived fluids and partial melting in subduction

zones: insights from two contrasting Mexican volcanoes (Colima and Ceboruco). *Journal of Volcanology and Geothermal Research*, **54**, 1–18.

Mercier J.L., Sébrier, M., Lavenu, A., Cabrera, J., Bellier, O., Dumont, J.-F. and Macharé, J., 1992. Changes in the tectonic regime above a subduction zone of Andean type; the Andes of Peru and Bolivia during the Pliocene-Pleistocene. *Journal of Geophysical Research*, **97**, 11945–11982.

McCulloch, M.T. and Gamble, J.A., 1991. Geochemical and geodynamical constraints on subduction zone magmatism. *Earth and Planetary Science Letters*, **102**, 358–374.

Martinez, C., 1980. Structure et évolution de la chaîne andine dans le nord de la Cordillére des Andes de Bolivie. ORSTOM, Travaux et documents, **119**, 352 p.

Nakamura, N., 1974. Determination of REE, Ba, Fe, Mg, Na and k in carbonaceous and ordinary chondrites. *Geochimica et Cosmochimica Acta*, **38**, 757–775.

Noble, D.C., Sébrier, M., Mégard, F. and McKee, E.H., 1985. Demonstration of two pulses of Palaeogene deformation in the Andes of Peru. *Earth and Planetary Science Letters*, **73**, 345–349.

Odin, G.S., 1994. Geological time scale. *Compte Rendus de l'Académie des Sciences, Paris*, **318**, 59–71.

Oliver, R.A., Robinson, S., Vittoz, P. and Vivier, G., 1990. The method of Instrumental Activation Analysis as practised at the Institut Laüe-Langevin (ILL), together with the abundance of 16 elements in twenty one International standard reference materials measured by this method. *Internal ILL report*, 11 p.

Pearce, J.A. 1983. Role of the sub-continental lithosphere in magma genesis at active continental margins. In: *Continental basalts and mantle xenoliths* (edited by C.J. Hawkesworth and M.J. Norry), pp. 230–249. Shiva Publishing, Nantwich, UK, 262 p.

Poupeau, G., Labrin, E., Sabil, N., Bigazzi, G., Arroyo, G. and Vatin-Pérignon, N., 1994. Fission-track dating of 15 macusanites glass pebbles from the macusani volcanic field (SE Peru). *Nuclear Trace Radiation Measurements*, in press.

Price, R.C., Gray, C.M., Wilson, R.E., Frey, F.A. and Taylor, S.R., 1991. The effects of weathering on rare-earth elements. Y and Ba abundances in Tertiary basalts from southeastern Australia. *Chemical Geology*, **93**, 245–265.

Redwood, S.D., 1987. The Soledad caldera, Bolivia: a Miocene caldera with associated epithermal Au-Ag-Cu-Pb-Zn mineralization. *Geological Society of America Bulletin*, **99**, 395–404.

Redwood, S.D. and Macintyre, R.M., 1989. K-Ar dating of Miocene magmatism and related epithermal mineralization of the northeastern Altiplano of Bolivia. *Economic Geology*, **84**, 618–630.

Schmitt-Riegraf, C. and Pichler, H., 1988. Cenoaoic ignimbrites of the Central Andes: a new genetic model. In: *The Southern Central Andes* (edited by H. Bahlburg, Ch. Breitkreuz and P. Giese), Lecture Notes in Earth Sciences, **17**, pp. 183–197. Springer-Verlag, Berlin, Germany, 261 p.

Sébrier, M., Lavenu, A., Fornari, M. and Soulas, J.-P. 1988. Tectonics and uplift in Central Andes (Peru, Bolivia and Northern Chile) from Eocene to Present. *Géodynamique*, **3**, 85–106.

Sempéré, T., Hérail, G., Oller, J. and Bonhomme, M.G., 1990. Late Oligocene-early Miocene major tectonic crisis and related basins in Bolivia. *Geology*, **18**, 946–949.

Sempéré, T., Baby, P., Oller, J., and Hérail, G., 1991. La nappe de Calazaya: une preuve de raccourcissements majeurs gouvernés par des éléments paléostructuraux dans les Andes boliviennes. *Compte Rendus de l'Académie des Sciences, Paris*, **312**, 77–83.

de Silva, S.L., 1989. Geochronology and stratigraphy of the ignimbrites from the 21°30×S to 23°30×S portion of the Central Andes of northern Chile. *Journal of Volcanology and Geothermal Research*, **37**, 93–131.

de Silva, S.L., Davidson, J.P., Croudace, A.W. and Escobar A., 1993. Volcanological and petrological evolution of Volcan Tata Sabaya, SW Bolivia. *Journal of Vocanology and Geothermal Research*, **55**, 305–335.

de Silva, S.L. and Francis, P.W. 1989. Correlation of large ignimbrites-two case studies from the Central Andes of northern Chile. *Journal of Volcanology and Geothermal Research*, **37**, 133–149.

de Silva, S.L. and Francis, P.W. 1991. *Volcanoes of the Central Andes*. Springer-Verlag, Heidelberg, Germany, 216 p.

Smith, D.R. and Leeman, W.P., 1993. The origin of Mount St. Helens andesites. *Journal of Volcanology and Geothermal Research*, **55**, 271–303.

Sparks, R.S.J., Self, S. and Walker, G.P.L. (1973). products of ignimbrite eruptions. *Geology*, **1**, 115–118.

Storzer, D. and Poupeau, G. 1973. Ages-plateaux de verres et minéraux par la méthode des traces de fission. *Compte Rendus de l'Académie des Sciences, Paris*, **276**, 137–139.

Thorpe, R.S., Francis, P.W. and Moorbath, S., 1979. Rare earth and strontium isotope evidence concerning the petrogenesis of north Chilean ignimbrites. *Earth and Planetary Science Letters*, **42**, 359–367.

Thorpe, R.S., Francis, P.W. and O'Callaghan, L. 1984. Relative soles of source composition, fractional composition and crustal contamination in the petrogenesis of Andean volcanic rocks. *Philisophical Transactions of the Royal Society of London*, **A310**, 305–320.

Toribio, P. 1899. Sinopsis de los tremblores y volcanes del Perú. **III**.- Erupción del Huaina-Putina en 1600. *Boletín della Societá Geografica de Lima*, **9**, 67–68.

Tosdal, R.M., Farrar, E. and Clark, A.H., 1981. K-Ar geochronology of the late cenozoic volcanic rocks of the Cordillera Occidental, Southernmost Perú. *Journal of Volcanology and Geothermal Research*, **10**, 157–173.

Vatin-Pérignon, N., Vivier, G., Sébrier, M. and Fornari, M. 1982. Les derniers événements andins marqués par le volcanisme cénozoïque de la Cordillére occidentale sud-péruvienne et de son piémont pacifique entre 15°45× et 18°S. *Bulletin de la Société Géologique de France*, (7) **24**, 679–650.

Wark, D.A., 1991. Oligocene ash flow volcanism, northern Sierra Madre Occidental: role of mafic and intermediate-composition magmas in rhyolite genesis. *Journal of Geophysical Research*, **96**, 13389–13411.

von Weibel, M., Frangipane-Gysel, M. and Hunziker, J., 1978. Ein beitrag zur Vulkanologie Süd-Perus. *Geologische Rundschau*, **67**, 243–252.

Wörner, G., Moorbath, S. and Harmon, R.S., 1992. Andean Cenozoic volcanic centers reflect basement isotopic domains. *Geology*, **20**, 1103–1106.

APPENDIX

Fission-Track Experimental Procedures

We collected three obsidian samples with a diameter of ~2 cm from the upper unit of the SA tuff, in the qda Añas Huayco near Arequipa for determining fission track ages. We have adopted for the fission-track dating of obsidian samples one of the approaches recommanded by the International Union of Geological Sciences, subcommission on Geochronology (Hurford, 1990) for the "population" method. Our procedures, justified in Bigazzi *et al.* (1988), are numerically equivalent to the onc using the zeta calibration (Hurford and Green, 1983).

One of several mm-sized fragments of each sample was irradiated in the well thermalized position P1 of the Orphée nuclear reactor of the Centre d'Etudes Nucléaires of Saclay. The neutron fluence was monitored from the induced fission track densities measured in freshly cleaved mica muscovite sheets maintained in contact with NIST reference wafer glass 962a during irradiation. n glass wafers were used, each of which sandwiched between 2 muscovite sheets. After irradiation, tracks were etched in HF 40% for 70 mn at 20°C. Track counts were made with a dry ×100 objective and ×10 oculars.

Apparent ages were determined with the "difference" technique (Gleadow, 1981), into which no laboratory heating treatment to erase fossil tracks is applied to the samples before irradiation. After irradiation, two fragments of each sample, respectively irradiatcd and non-irradiated, are mounted together in araldite and polished. Tracks were etched with HF 20% at 20°C for 90 seconds. Track counts were made either with an Orthoplan or a Jenavert-Zeiss Jena microscope with a ×100 dry objective and ×10 oculars. Track size was characterized by the measurements of track diameter, defined as the largest linear dimension of a track.